Ola Zeidan [1]
Walid Sahyouni [1]
Alaa Nassif [2]

[1] Department of Physics, Homs University, Homs, SYRIA
[2] Faculty of Pharmacy, Al-Wataniya Private University, Hama, SYRIA

Loss of Helium Ions Energy Emitted by Plasma Focus within Tungsten

The research aims to study the loss of helium ions energy emitted by plasma focus within tungsten, which is one of the most widely used materials in the vacuum chamber of plasma focus devices and nuclear fusion reactors. First, the characteristics of the plasma focus formed when helium gas pressure changes were determined, and then the characteristics of the helium ion beam emitted by the NX2 dense plasma focus device were determined using Lee code. Then perform a simulation of helium ions interaction within a 1 μm thickness of tungsten at three values of helium ion energy 76, 131, and 204 keV, and determine penetration depth of ions, then use SRIM to determine ion energy loss values. The results showed the formation of bulges within the tungsten due to the assembly of helium ions due to loss their energy with the tungsten electronic cloud.

Keywords: Plasma focus; Helium ions; Lee code; SRIM
Received: 26 February 2025; **Revised:** 15 April 2025; **Accepted:** 22 April 2025

1. Introduction

Dense Plasma Focus (DPF) is a type of electrical discharge within plasmas with densities $n>10^{19}$ cm^{-3} and temperatures of several kiloelectronvolts over a period of time of 100 to 150 ns, and at the end of it, a very hot and dense plasma column "pinch" is formed near or at the end of anode located in the center of the vacuum chamber, where part of the magnetic energy stored in the tube (vacuum chamber) and the external circuit (capacitor bank) is converted rapidly into the plasma during the short collapse of the current sheath toward the chamber axis [1], then plasma instabilities lead to collapse of formed plasma pinch. Since the discovery of this physical phenomenon in the early 1960s by Mather [2] and Filippov [3], plasma focus devices have been used as an ion source for many applications such as the deposition of thin films [4], material processing [5], production of short-lived radioactive isotopes [6].

These devices also played a major role in nuclear fusion research at lower cost than experimental reactors, as they were used as a simulation model for the behavior of materials under nuclear fusion conditions, where they emit ions with an energy of up to several hundred keV and a temperature of 0.1-1 keV and energy density reaches more than 10^{12} W/cm^2 [7]. Under these conditions, materials used in fusion reactors are tested, as the main challenge in achieving fusion power is selecting materials for the various components of the thermonuclear fusion reactor, the most important of these components is the inner wall of the reactor, which will be exposed to thermal loads in the form of energy ions and electromagnetic radiation [8]. The thermal load can reach 0.5 MW/m^2, and plasma disturbances to energy densities up to tens of MJ/m^2 for periods of up to 1 ms, which leads to a lead to change in structural properties of inner wall material. Therefore, there are very strict requirements for the properties of the materials that will be exposed to the plasma, such as high thermal conductivity, good mechanical properties, and resistance to radiation damage, so It is necessary to understand the behavior of these materials under conditions similar to those found in fusion reactors, which helps in selecting them and developing new materials.

Tungsten is one of good materials to use in the inner wall of fusion reactors due to its unique properties such as high melting point, great resistance to friction, and low amount of activation due to exposure to neutrons [9,10]. In this context, many actual and simulation experiments have been conducted of exposing tungsten to ion beams emitted by plasma focus, including using plasma focus device with operating power 2.2 kJ to expose tungsten plates to protons using multiple shots by Bhuyan and others, and they observed various damage features such as small cracks on tungsten surface after irradiation [11]. Dutta and others [12] also used a 2.2 kJ plasma focus device to study the changes caused by the helium ion in tungsten and study the characteristics of surface damage.

2. Energy Loss of Ions within Material

When the ion moves through a target at a certain depth, it loses its energy to the target, where the stopping power is given by [13]:

$$\frac{dE}{dx} = -n.S(E) \qquad (1)$$

where dE is the energy loss of ions moving through the target with density n, dx is the thickness of the target, $S(E)$ is the cross section of atomic stop and it contains two components: electronic S_e and nuclear S_n

Electronic stopping power is the process in which the ion arriving at the target is lost its energy to target electrons through a number of processes such as the electron- electron collisions , excitation or ionization of the target atoms, or ionization of conduction electrons, where target electrons can be exposed to inelastic collisions and become ionized or excited [13]. The electronic stopping power is calculated using Bethe-Bloch [14]:

$$-\frac{dE}{dx} = n.S_e(v) \quad (2)$$

where n is the number density of scattering centers and $S_e(v)$ is the stopping cross section as a function of the ion velocity:

$$S_e(v) = \frac{4\pi e^4 Z^4}{mv^2} \ln\frac{2mv^2}{I} \quad [eV\ m^2] \quad (3)$$

where e and m are charge and mass of the electron, Z is ion charge , and I is the average excitation potential of the target

It is clear that the electronic stopping power depends on the constantly changing of ion speed as the ion penetrates the target and is stripped of some its electrons, which leads to its charge becoming dependent on the target.

Unlike electronic stopping power, nuclear stopping power is in discrete quantities. Nuclear stopping depends on coulomb potential between atoms nuclei, which includes all processes in which of ion energy as a whole is transferred to the target through elastic collisions. Coulomb potential U is given by:

$$U = \frac{Z_p Z_t}{r} \quad (4)$$

Where Z_p and Z_t are atomic numbers of the projected atom and the target atom, respectively, r is the distance between the nucleus. The differential cross section of Columb scattering is given by [15]:

$$\frac{d\sigma}{d\Omega} = \left(\frac{Z_p Z_t e^2}{4E_0 \sin^2\frac{\theta}{2}}\right)^2 \quad (5)$$

Where E_0 is the initial kinetic energy of ion, and θ is the deflection angle

We studied the interaction of helium ions emitted by the NX2 dense plasma focus device within tungsten and discussed the mechanisms of loss of ion beam energy by studying formed plasma focus and the changes in characteristics of emitted ions beam with a helium pressure changes , and then its interaction with tungsten and calculating the nuclear and electronic stopping power.

3. Results

3.1 Properties of plasma focus changes with helium pressure changes

Lee's code was used to find the plasma focus characteristics formed within NX2 dense plasma focus device with an operating energy 2.7 kJ when helium gas pressure changes until the pressure value beyond which focus does not occur, in order to determine the specifications of plasma focus, which is considered a source of helium ions, and the results were as follows:

3.2 Changes of the characteristics of ion beam when helium pressure changes:

The of the helium ion beam characteristics emitted after plasma pinch collapse were found to determine the flux, energy, number of ions, and the value of beam energy flux (thermal component $W.m^{-2}$), and the results were the following:

3.3 Penetration of helium ions into tungsten:

After finding the ions beam characteristics, the energy of helium ion interacting with tungsten was found, as it was within the energy range 76-204 keV. Three values were chosen for ion energy, 76 keV. 131 keV, 204 keV and finding the penetration range of ions within a thickness of 1 µm of tungsten using the Transport of Ions in Matter TRIM program according to the following:

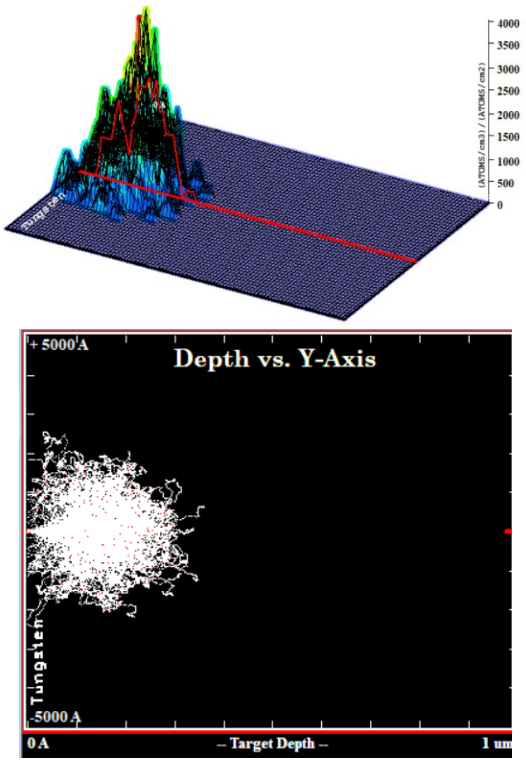

Fig. (1) Helium ions with energy 76 keV within tungsten

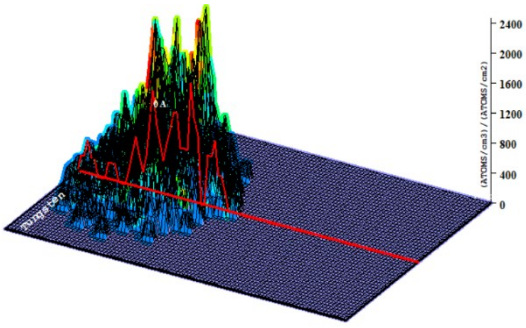

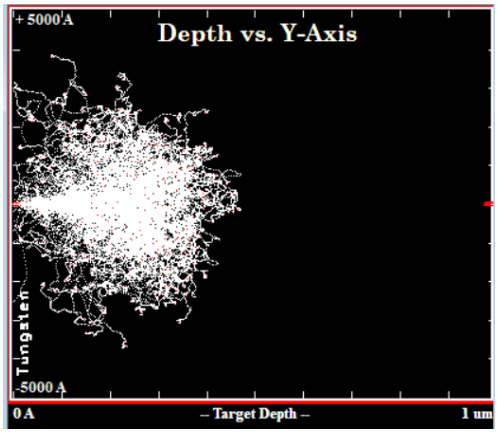

Fig. (2) Helium ions with energy 131 keV within tungsten

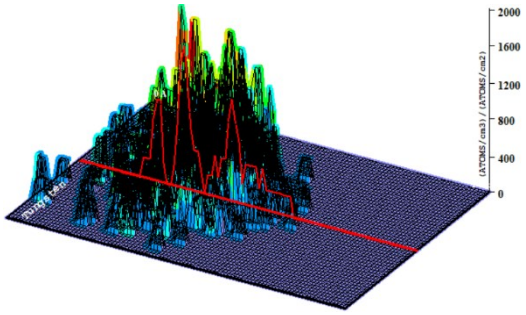

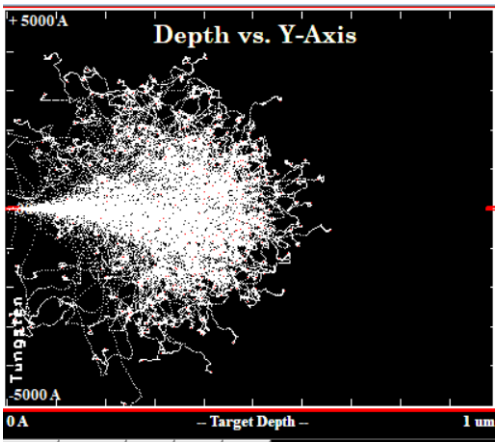

Fig. (3) Helium ions with energy 204 keV within tungsten

We used SRIM to calculate nuclear and electronic stopping powers within the energy range of the helium ions 76-204 keV and the following results were:

4. Discussion

We notice an increase of ions penetration into tungsten with increasing ion energy, as the range of the ions was 1685Å, 2594Å, and 3683Å, respectively, in addition to increasing the area of their diffusion . The red dots indicate the tungsten atoms that were displaced by helium ions, as we notice their very low number, and the white area indicates the accumulation of helium ions. This explains the presence of bulges within the tungsten resulting from local accumulations of helium ions, which increase with the increase of ions energy. Therefore, it can be said that helium ions interact with the electronic cloud of tungsten atoms for the most part, with a very small number of interactions with the nuclei. We note the very high value of electronic stopping power compared to nuclear one, as it can be neglected, and this is what confirmed our results that the loss of most of helium ions energy is due to collisions with the electron cloud of the tungsten atom and not with the nuclei.

Table (3) Nuclear and electronic stopping power of helium ions within tungsten

Ion Energy (keV)	dE/dx electronic (eV/Å)	dE/dx Nuclear (eV/Å)
80	34.3595	0.8095
90	36.5031	0.7631
100	38.5522	0.7622
110	40.4068	0.6868
120	42.1949	0.6549
130	43.8863	0.6263
140	45.4905	0.6005
150	47.0171	0.5771
160	48.4656	0.5556
170	49.846	0.536
180	51.1479	0.5179
200	53.5856	0.4856
204	54.0495	0.4795

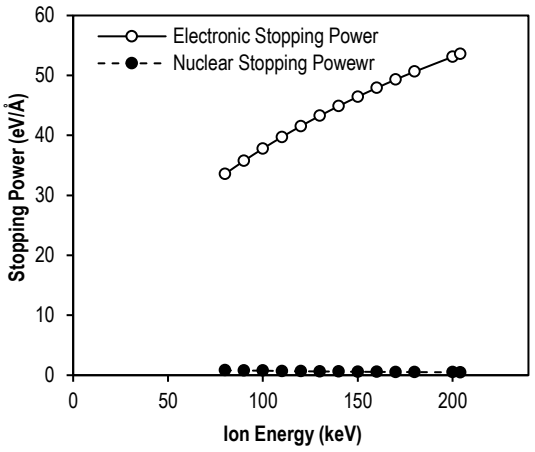

Fig. (4) Nuclear and electronic stopping power as a function of helium ion energy

5. Conclusions

The results of this research provided an idea of the damage occurring in the inner wall material of fusion reactor made of tungsten as a result of exposure to helium ions and an explanation for emerging bulges. It also demonstrated the importance of dense plasma focus devices as simulators for testing the behavior of materials under nuclear fusion conditions.

References

[1] S.R. Chung, R.A. Behbahani and C. Xiao, "Charged particles and x-ray emission studies on a

dense plasma focus device", *Rad. Effects Defects Solids*, 175(11-12) (2020) 1015-1020.
[2] J.W. Mather, "Formation of a high-density deuterium plasma focus", *The Phys. Fluids*, 8(2) (1965) 366-377.
[3] V.F. D'yachenko V.S. Imshennik, "Two-Dimensional Magnetohydrodynamic Model for the Dense Plasma Focus of AZ Pinch", in Reviews of Plasma Physics/Voprosy Teorii Plazmy, Springer (Boston, 1980), pp. 199-299.
[4] R.S. Rawat et al., "Nano-phase titanium dioxide thin film deposited by repetitive plasma focus: Ion irradiation and annealing based phase transformation and agglomeration", *Appl. Surf. Sci.*, 255(5) (2008) 2932-2941.
[5] J.N. Feugeas et al., "Nitrogen implantation of AISI 304 stainless steel with a coaxial plasma gun", *J. Appl. Phys.*, 64(5) (1988) 2648-2651.
[6] A. Nassif et al., "Determination of conditions for obtaining radioactivity of nitrogen-13 isotope for medical use by NX2 dense plasma focus device", Научно-технические ведомости Санкт-Петербургского государственного политехнического университета. Сер.: Физико-математические науки, (2023) 16(2).
[7] V.A. Gribkov et al., "Interaction of high temperature deuterium plasma streams and fast ion beams with stainless steels in dense plasma focus device", J. Phys. D: Appl. Phys., 36(15) (2003) 1817.
[8] J.N. Brooks et al., "Plasma–surface interaction issues of an all-metal ITER", *Nucl. Fusion*, 49(3) (2009) 035007.
[9] B.B. Cipiti and G.L. Kulcinski, "Helium and deuterium implantation in tungsten at elevated temperatures", *J. Nucl. Mater.*, 347(3) (2005) 298-306.
[10] S. Takamura et al., "Investigation on the effect of temperature excursion on the helium defects of tungsten surface by using compact plasma device", *J. Nucl. Mater.*, 415(1) (2011) S100-S103.
[11] M. Bhuyan et al., "Plasma focus assisted damage studies on tungsten", *Appl. Surf. Sci.*, 264 (2013) 674-680.
[12] N.J. Dutta, N. Buzarbaruah and S.R. Mohanty, "Damage studies on tungsten due to helium ion irradiation", *J. Nucl. Mater.*, 452(1-3) (2014) 51-56.
[13] J.F. Ziegler, M.D. Ziegler and J.P. Biersack, "SRIM–The stopping and range of ions in matter", *Nucl. Instrum. Meth. Phys. Res. B: Beam Interact. Mater. Atoms*, 268(11-12) (2010) 1818-1823.
[14] S.P. Sauer, J. Oddershede and J.R. Sabin, "Theory and Calculation of Stopping Cross Sections of Nucleobases for Swift Ions", in **Radiation Damage in Biomolecular Systems**, Springer Netherlands (Dordrecht, 2011), pp. 191-200.
[15] E. Rutherford, "The scattering of α and β particles by matter and the structure of the atom", *Philo. Mag.*, 92(4) (2012) 379-398.

Table (1) Characteristics of plasma focus when the helium pressure changing in NX2

Pressure (Torr)	Peak current I_{peak} (kA)	Pinch current I_{pinch} (kA)	Plasma Temperature T_e (×10⁶ K)	Pinch radius r_p (cm)	Pinch Length z_p (cm)	Pinch duration τ (ns)	Induced voltage V_{max} (kV)	Plasma density N_i (×10²³/m³)
1	270	162	11.9	0.30	2.876	14.3	34	0.9
2	310	185	7.7	0.30	2.876	17.8	31	1.8
3	334	197	5.9	0.31	2.875	20.4	29	2.7
4	350	206	4.8	0.31	2.877	22.6	27	3.6
5	362	211	4.0	0.31	2.874	24.6	26	4.4
6	371	215	3.5	0.31	2.875	26.5	24	5.3
7	379	218	3.1	0.31	2.875	28.3	23	6.1
8	385	220	2.7	0.32	2.873	29.9	22	6.9
9	389	221	2.5	0.32	2.875	31.6	21	7.6
10	393	222	2.2	0.32	2.872	33.2	20	8.4
11	397	222	2.0	0.32	2.872	34.9	19	9.1
12	399	221	1.8	0.32	2.872	36.5	18	9.7
13	402	221	1.7	0.33	2.871	38.2	17	10.4
14	404	220	1.6	0.33	2.870	39.9	16	11.0
15	406	218	1.4	0.33	2.867	41.6	16	11.5
16	408	217	1.3	0.34	2.866	43.1	15	12.1
17	410	215	1.2	0.34	2.866	44.9	14	12.5
18	412	213	1.1	0.34	2.864	46.7	13	13.0
19	413	210	1.1	0.35	2.863	48.6	13	13.3

Table (2) Ion beam characteristics when helium pressure changing in NX2

Pressure (Torr)	Ions Flux J_b ($\times 10^{27}$ ions. $m^{-2}s^{-1}$)	Energy flux ($\times 10^{14}$ W.m^{-2})	Ions Beam Energy E_b (J)	Ions Number
1	3.2E+27	1.0E+14	43.0	1.3E+15
2	4.3E+27	1.3E+14	66.1	2.2E+15
3	5.0E+27	1.4E+14	83.3	3.0E+15
4	5.5E+27	1.4E+14	97.0	3.7E+15
5	5.9E+27	1.5E+14	108.0	4.4E+15
6	6.2E+27	1.5E+14	117.2	5.0E+15
7	6.5E+27	1.4E+14	124.6	5.6E+15
8	6.6E+27	1.4E+14	130.5	6.2E+15
9	6.8E+27	1.4E+14	135.5	6.8E+15
10	6.9E+27	1.3E+14	139.2	7.3E+15
11	6.9E+27	1.3E+14	142.4	7.8E+15
12	6.9E+27	1.2E+14	144.5	8.4E+15
13	6.9E+27	1.1E+14	145.8	8.9E+15
14	6.9E+27	1.1E+14	146.9	9.4E+15
15	6.8E+27	1.0E+14	146.9	9.8E+15
16	6.7E+27	9.5E+13	146.2	1.0E+16
17	6.6E+27	8.9E+13	145.2	1.1E+16
18	6.4E+27	8.3E+13	143.7	1.1E+16
19	6.3E+27	7.7E+13	141.8	1.2E+16

